Indian Journal of Marine Sciences
Vol. 19, June 1990, pp. 79-82

Diffraction of long period water waves around Mauritius island

P Chandramohan, B U Nayak & N Patil
National Institute of Oceanography, Dona Paula, Goa 403 004, India

Received 11 July 1989; revised 12 January 1990

Using Green's function, the Helmholtz equation with Sommerfeld condition has been solved numerically, to compute the diffracted wave potentials in a wave field. Software DIFIS is developed to evaluate the diffracted wave field around the Mauritius island for the storm waves arriving from south, southeast and east directions. The diffraction coefficients exceed 1.5 along the southern and eastern sides, and they vary between 0.4 and 0.9 along the western side of the Mauritius Island. The effect of diffraction is negligible for the wave periods exceeding 600 s.

The waves while propagating from deep water to the coast, undergo changes in wave height, direction and celerity due to shoaling, refraction, bottom friction and diffraction[1]. The diffraction of water wave is a phenomenon in which the energy is transferred laterally along the wave crest and it occurs when a chain of waves is interrupted by a barrier. In case of offshore islands, the study on the diffraction of long period waves such as tsunamis, tidal waves, storm surges, wind set up, etc. is very important in protecting the coasts from flooding and inundation. Using different methods, studies have been made in order to understand the diffraction around large cylinders and islands[2-12]. In the present study, a software for diffraction around island (DIFIS) has been developed for numerically solving the diffraction equations and has been used for estimating the diffracted wave field around the Mauritius island.

Study Area

Mauritius island is situated in the southern tropical belt of Indian Ocean, about 800 km east of Madgascar island, and at the south end of a long submarine ridge that extends from Seychelles (Fig. 1). It is approximately elliptical in shape, with a coastline of 200 km. As most of the shoreline was reached by the lava flows, sea cliff exists only where coral reefs are absent, in sector along the south and west coasts. Elsewhere reefs, reef flats and lagoons are present with varying width. The waves show monthly mean significant wave height around 2 m except June to August, during which they exceed 2.5 m. The monthly average zero crossing wave period varies between 8 and 9 s. During cyclonic days and high spring tide, rise in water level considerably increases the wave activities on the inland beaches. The tides in this region is of semidiurnal type, with an approximate spring tidal range of 45 cm, and neap tidal range of 10 cm. Mauritius island receives more than 80% of the wind from southeast and east and occasionally from other directions. Mauritius island is situated in the Inter-Tropical Convergence Zone, which is often exposed to tropical cyclones in the southwest Indian Ocean.

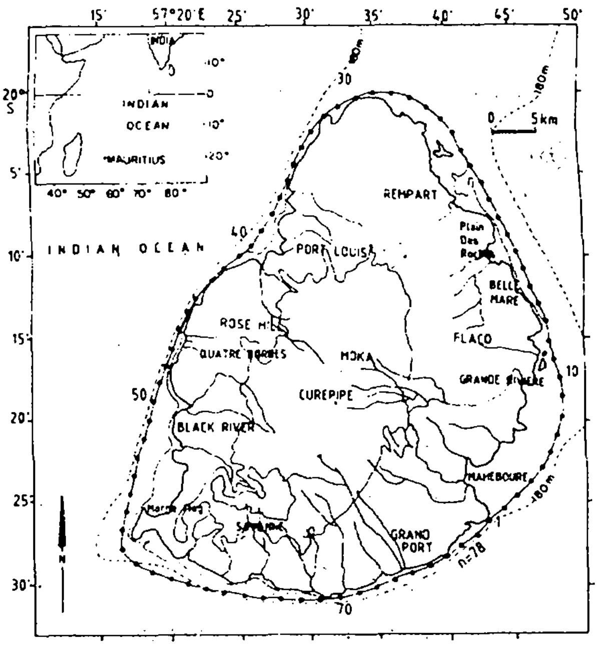

Fig. 1 – Location map

Methods

Governing equations—When the wave field is defined as shown in Fig. 2A, based on linear wave theory, the governing equations for diffraction analysis are given by,

(i) Helmholtz equation:

$$\nabla^2 \phi_D + k^2 \phi_D = 0 \qquad \ldots (1)$$

where, $\nabla^2 = (\partial^2/\partial x^2) + (\partial^2/\partial y^2) + (\partial^2/\partial z^2)$, ϕ_D = diffracted wave potential, k = wave number = $2\pi/L$ and L = wave length.

(ii) Sommerfeld radiation condition:

$$\lim_{r\to\infty}, r^{1/2}[(\partial\phi_D/\partial r) - ik\phi_D] = 0 \qquad \ldots (2)$$

where, r = distance of the point and $i = \sqrt{-1}$.

(iii) Boundary condition:

$$(\partial\phi_D/\partial n) = -(\partial\phi_I/\partial n) \qquad \ldots (3)$$

where, n = normal to surface and ϕ_I = incident wave potential.

Solution:

The boundary value problem governed by above Eqs 1-3 are solved by the method of Green's function[13]. Following the Weber's solution to the Helmholtz equation[13,14], the diffracted wave potential for any point P, exterior to the bounding curve C is given by (Fig. 2B),

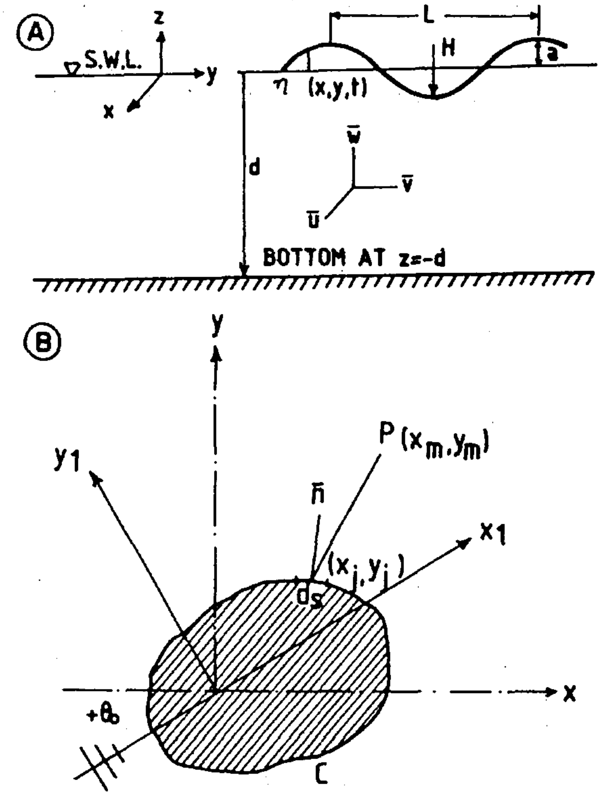

Fig. 2 – Definition sketch for: (A) fluid motion and (B) structure (terms are explained in text)

$$\phi_D(p_m) = (i/4) \int \left[\phi_D(s) \frac{\partial H_0^1(kr)}{\partial n} - H_0^1(kr) \frac{\partial \phi_D(s)}{\partial n} \right] ds \qquad \ldots (4)$$

where, $\phi_D(p_m)$ = diffracted wave potential at exterior point P_m (Fig. 2B), $\phi_D(s)$ = diffracted wave potential on the surface C, $r = [(x_m - x_j)^2 + (y_m - y_j)^2]^{1/2}$, the distance from the point (P_m) to any point (P_j) on the body, ds = incremental arc length on the body curve C, $H_0^1(kr) = J_0(kr) + iY_0(kr)$, the Hankel function of the first kind and zeroth order, J_0 = Bessel function of first kind and zeroth order, Y_0 = Bessel function of second kind and zeroth order.

Harms[13] has presented solution in numerical form for Eq. 4 to determine the diffracted wave potential along the boundary and at far field as,

$$p[1 - (\alpha/2\pi)] = (k/4) \int_c [p(s)\, Y_1(kr) + q(s) J_1(kr)] r_n ds + (1/4) \int_c [u(s)\, Y_0(kr) + v(s) J_0(kr)] ds \qquad \ldots (5)$$

$$q[1 - (\alpha/2\pi)] = (k/4) \int_c [q(s)\, Y_1(kr) - p(s) J_1(kr)] r_n ds + (1/4) \int_c [v(s)\, Y_0(kr) - u(s) J_0(kr)] ds \qquad \ldots (6)$$

where, p and q = components of diffracted wave potential at a point (x_m, Y_m), J_1 = Bessel function of first kind and first order, Y_1 = Bessel function of second kind and first order, α = interior angle at point m.

The integration is performed with respect to point (x_m, Y_m). The radius vector r originates from this point and extends to a point (x_j, Y_j) on the body surface (Fig. 2B). Eqs 5 and 6 are written in the form of finite sums over the n number of elementary boundary lengths as,

$$p[1 - (\alpha/2\pi)] = (k/4) \sum_{j=1}^{n} [p_j Y_1(kr_{jm}) + q_j J_1(kr_{jm})](r_n)_{jm} A_j + (1/4) \sum_{j=1}^{n} [u_j Y_0(kr_{jm}) + v_j J_0(kr_{jm})] A_j \qquad \ldots (7)$$

$$q[1 - (\alpha/2\pi)] = (k/4) \sum_{j=1}^{n} [q_j Y_1(kr_{jm}) - p_j J_1(kr_{jm})](r_n)_{jm} A_j + (1/4) \sum_{j=1}^{n} [v_j Y_0(kr_{jm}) - u_j J_0(kr_{jm})] A_j \qquad \ldots (8)$$

where, p_j and q_j = components of diffracted potential at point, (x_j, Y_j), α = interior angle at a point m, A_j = arc length s_j associated with point m, r_{jm} = radius vector from a point m to general point j on the boundary,

$$r_{jm} = |r_{jm}| = [(x_j - x_m)^2 + (y_j - y_m)^2]^{1/2}$$

$$(r_n)_{jm} = (1/r_{jm})[r_{jm} \cdot n]$$

$$= (1/r_{jm})[(x_j - x_m)(y_s)_j - (y_j - y_m)(x_s)_j]$$

$$(x_s)_j = [x_{j+1} - x_j]/ds_j = \cos\beta$$

$$(y_s)_j = [y_{j+1} - y_j]/ds_j = \sin\beta$$

$u(t) = k \sin kx_1 \cdot \sin\beta$ velocity in x direction

$v(t) = k \cos kx_1 \cdot \sin\beta$ velocity in y direction

$x_1 = x\cos\theta_0 + y\sin\theta_0$ is evaluated at point j

θ_0 = angle of wave approach with respect to x axis

From the estimated values of p and q using Eqs 7 and 8, the diffraction coefficients at all n points on the boundary are determined by,

$$K_m = [(p + \cos kx_1)^2 + (q + \sin kx_1)^2]^{1/2} \quad \ldots (9)$$

where, K_m = diffraction coefficient at point m,

Software DIFIS is developed, to numerically solve Eqs 7 and 8, to estimate diffracted wave potential components p and q at all n points along the boundary, and for the far away points. Eq. 9 is then, used to estimate the diffraction coefficients at points under consideration.

The assumptions made in arriving at solutions are, (i) island is situated in an infinite ocean of constant water depth (ii) flow is irrotational (iii) fluid is inviscid and incompressible (iv) incoming wave trains are unidirectional, monochromatic and sinusoidal, and (v) effect of bottom friction close to the shore is negligibly small.

Results and Discussion

The software DIFIS was used to estimate the diffracted wave field for a circular island and the results are compared with analytical solution presented by Banaugh[15]. Values estimated by the numerical procedure agree very well with the analytical results (Fig. 3), the variation being within 8 to 10%, which is reasonable in numerical analysis, in view of various assumptions made and techniques adopted in numerical solutions.

The curvature of the coastal boundary of the island is smooth, and it is divided into 78 equal elementary segments (Fig. 1). Cyclonic storms, frequently approach Mauritius island from the southeast. The variation of diffraction coefficients along the coastline, for the southeasterly waves, of periods 120, 180, 240, 300, 360, 420 and 600 s are shown in Figs 4 and 5.

The diffraction coefficient along the boundary of coastline varies between 0.8 and 2.5 for the waves from 150 to 180 s. It steadily varies between 0.3 and 2 for the waves of 240 s, between 0.8 and 2 for the waves

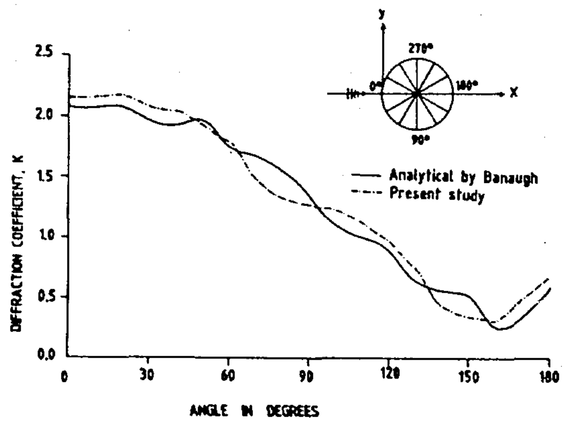

Fig. 3 – Diffraction coefficient around circular island

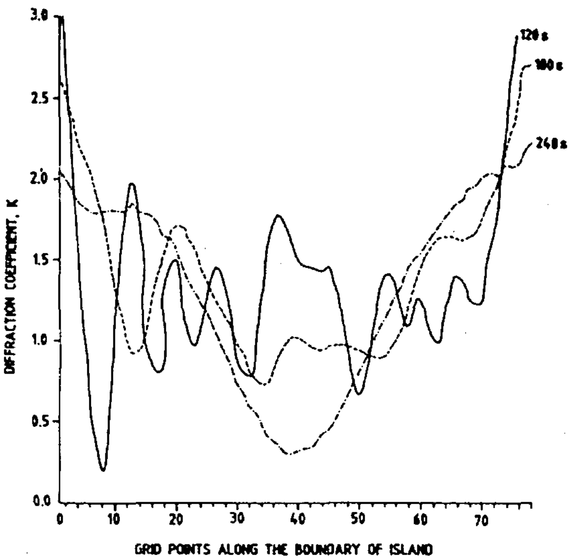

Fig. 4 – Diffraction coefficient around Mauritius island

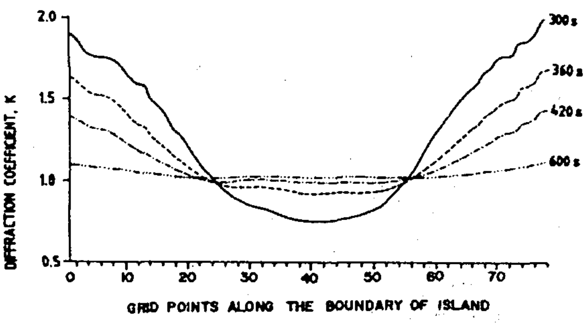

Fig. 5 – Diffraction coefficient around Mauritius island

of 300 s, between 1 and 1.5 for the waves of 360 s, and between 1 and 1.4 for the waves of 420 s. As the influence of diffraction was found to be negligible for the waves having period less than 100 s and above 600 s, the present study has been made for the wave periods between 120 and 600 s. Mauritius coast, however at times, experiences storm waves with period varying from 120 to 600 s.

The variation of diffraction coefficients, over the surrounding waters off the island are estimated for the waves of 240 s, arriving from south, southeast, and east, and the results are presented in Fig. 6. For southeasterly and easterly waves, the influence of diffraction on the south coast is high, varying between 1.2 and 2. The effect is significant along the east coast, with diffraction coefficients varying between 1 and 1.5. West coast, forming the leeward side of the wave approach, is subjected to low values of diffraction coefficients varying between 0.4 and 0.9. Consequently, for southerly waves, the entire coastline except the northern tip, is exposed to high values of diffraction coefficients exceeding 1.

The present results are subject to certain limitations, owing to various assumptions involved in the diffraction theory and the method of numerical analysis. However, the results based on the present model for the circular islands closely agree with the theoretical results.

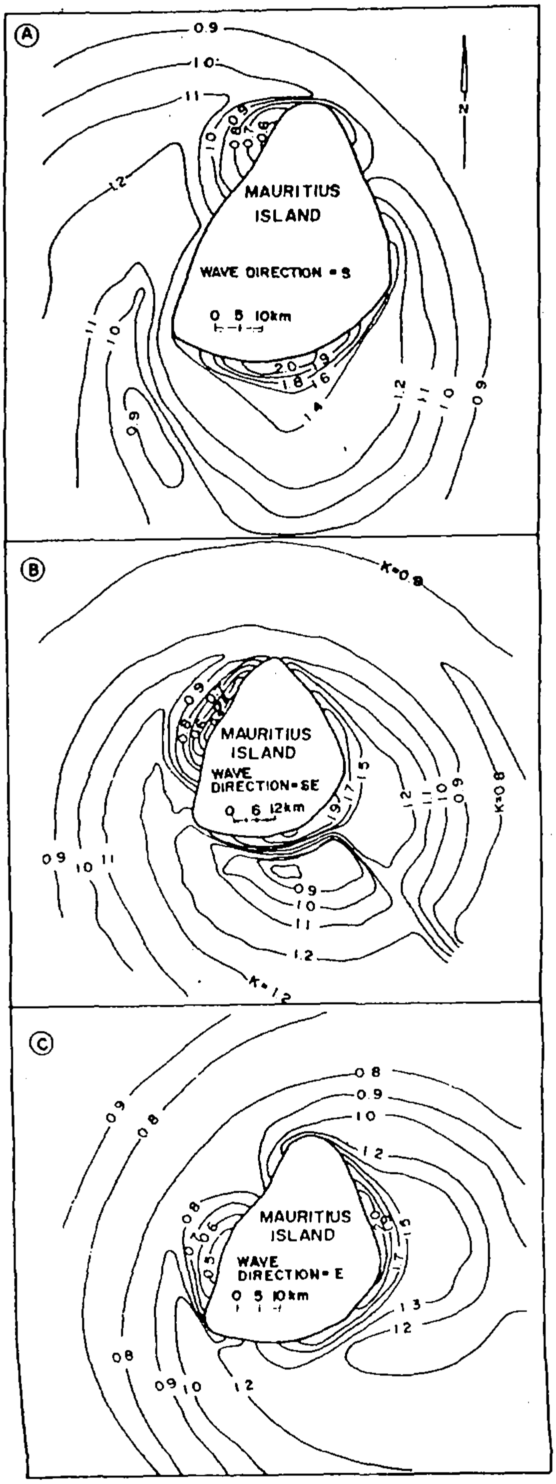

Fig. 6 – Diffraction wave field for: (A) southerly waves, (B) southeasterly waves and (C) easterly waves

Acknowledgement

Authors are thankful to Dr. B.N. Desai, Director, for the encouragement, Mr. S. Ragoonaden, Mauritius Mateorological Services, Vacoas and Dr. R. Mahadevan, Indian Institute of Technology, Madras for their help.

References

1 Ippen A T, *Estuary and coastline hydrodynamics*, (McGraw Hill, New York) 1966, pp. 744.
2 Mei C C, *Ann Rev Fluid Mech*, 10 (1978) 393.
3 Jonsson I G, Skovgaard O & Kjaer B, *J Mar Res*, 34 (1976) 469.
4 Vastano A C & Reid R O, *J Fluid Mech*, 25 (1967) 129.
5 Smith R & Sprinks T, *J Fluid Mech*, 72 (1975) 373.
6 Isaacson M, *J Waterways Port Coastal Ocean Engg Div ASCE*, 103 (1977) 69.
7 Berkhoff J C W, *Proc 13th Conf Coastal Engg ASCE*, 1 (1972) 471.
8 Christiansen P L, *Proc 14th Conf Coastal Engg ASCE*, 1 (1974) 601.
9 Lozano C & Liu P L, *J Fluid Mech*, 101 (1980) 705.
10 Ebersole B A, *J Waterways Port Coastal Ocean Engg Div ASCE*, 111 (1985) 939.
11 Sarpkaya T & Isaacson M, *Mechanics of wave forces on offshore structures*, (Van Nostrand Reinhold Co, New York), 1981, pp. 651.
12 Harms V W, *J Waterways Port Coastal Ocean Engg Div ASCE*, 105 (1979) 131.
13 MacCamy R C & Fuchs R A, *Tech Memorandum*, No. 69 (CERC, US Army, Washington, DC) 1954.
14 Sneddon I N, *Elements of partial differential equations*, (McGraw Hill Book Co Inc, New York) 1957, pp. 240.
15 Banaugh R P, *The scattering of acoustic and elastic waves by surfaces of arbitrary shape*, Ph.D thesis, University of California, 1962.